Electrophoretic Molecular Communication with Piecewise Constant Electric Field

Junseob Kim, Sunghwan Cho, *Member, IEEE,* Justin P. Coon, *Senior Member, IEEE,*
Alfonso A. Castrejón-Pita, and Hamidreza Arjmandi

Abstract—**This paper studies a novel electrophoretic molecular communication (EMC) framework utilizing a piecewise constant electric field. EMC is a particular type of molecular communication that exploits electric fields to induce the movement of charged particles to enhance communication performance. Our previous work proposed an EMC framework utilizing a time-varying electric field that exponentially changes; however, the field with such a complicated shape might be challenging to be implemented in practice. Thus, this paper proposes a new EMC approach exploiting a piecewise constant electric field that can be readily implemented via, e.g., an on/off switch method. We formulate two optimization problems to design the electric field based on different objectives: minimizing a mean squared error and minimizing a bit interval. The solutions of each, such as optimal on-off timings and corresponding strengths of the constant electric fields, are obtained through the Lagrange multiplier approach and the geometric programming, respectively. The Monte Carlo simulation results verify that the proposed piecewise constant electric field significantly reduces the bit error rate relative to the constant field benchmark while performing less well, but not significantly, than the exponential field benchmark.**

Index Terms—**Electrophoretic molecular communication, electrophoresis, nanonetworks, piecewise constant velocity**

I. INTRODUCTION

MOLECULAR communication (MC) is a bio-inspired communication approach technically harnessing molecular signaling in a fluid medium [1], [2]. MC devices communicate by modulating information in the number, type/structure, or release time of the information-carrying molecules, which is efficient and practical in various nano- or micro-scale applications. Traditional radio frequency (RF) or optical communications are impractical at such small extents because of the constraints that the antenna size for RF communications should be the scale of the signal's wavelength, and optical communications require either a guided medium or line of sight [3].

In MC systems, transferring the molecular information signals toward the destination (receiver) device mainly relies on the molecules' random diffusion and the advection of the channel's aqueous medium. By itself, diffusion is a very slow and noisy information transmission process. Hence, the flow advection is exploited to achieve higher performances, especially in an elongated channel environment [4]–[7].

Transport by advection is categorized as force-induced drift and bulk flow; the former induces advection by external forces acting on the information-carrying molecules, while the latter induces the flow of the entire channel medium. On the other hand, utilizing the bulk flow to transport the information-carrying molecules may not be suitable for applications where inducing a flow of the medium itself is problematic, unwanted, or even impossible. Thus, we recently proposed the new framework of electrophoretic molecular communication (EMC) utilizing an electric field to allow ideally charged information-carrying molecules to propagate in a direction independent of any fluid flow that may already exist in the channel medium [8]. The proposed electric field that changes as a form of exponential or sinusoidal function achieved a considerably better bit error probability (BER) performance by strengthening the molecular signaling and decreasing the intersymbol interference (ISI), compared to constant advection.

On the other hand, because of stringent hardware requirements of microscopic MC devices in terms of their dimensions, battery life, circuit complexity, etc., it might not be possible to implement such complicated time-varying electric fields in practical MC systems. Hence, this paper proposes and investigates a piecewise constant electric field, which would be much easier to be implemented via, e.g., an on/off switch methods, in reality. We formulate two optimization problems to design the electric field based on different objectives: minimizing a mean squared error (MSE) and minimizing a bit interval, while both are constrained by the average power of the field. The solutions of each, such as optimal on-off timings and corresponding values of the constant electric fields, are obtained through the Lagrange multiplier approach and the geometric programming (GP), respectively. We show that the optimized piecewise constant field significantly lowers the BER relative to typical constant advection but is slightly higher than that of the exponential field proposed in [8]; however, this observation can be considered a reasonable trade-off when considering the much more straightforward implementation complexity of the piecewise constant field.

: Information-carrying type-A molecule

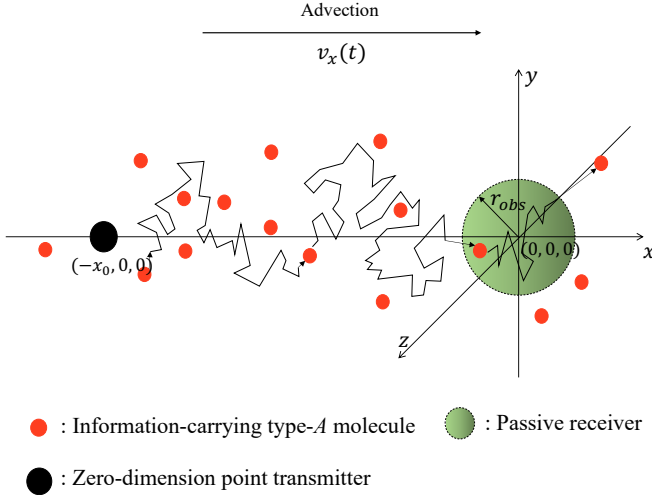: Passive receiver

: Zero-dimension point transmitter

Fig. 1. Schematic description of the system model, including a point transmitter, three-dimensional infinite channel, and a passive receiver sphere.

The rest of this paper is organized as follows. Section II describes the considered system model, including the mathematical received signal and detection models. Then, Section III investigates the optimization problems for obtaining the piecewise constant electric field parameters, and Section IV explains how the two designed electric fields function. In Section V, the numerical and simulation results are provided to validate our analysis, and Section VI concludes the paper.

II. SYSTEM MODEL

A. Transmitter

In this study, a three-dimensional fluid environment of constant uniform temperature and viscosity is considered, as described in Fig. 1. A point transmitter, i.e., a source of information molecules, is assumed to be located at $(-x_0, 0, 0)$, and a passive (transparent) receiver sphere with radius r_{obs} is assumed to be fixed at the origin $(0, 0, 0)$. The transmitter utilizes a binary modulation that uses only two symbols 0 and 1. To send bit 1, N_{EM} type-A information molecules are emitted, where N_{EM} is the number of the molecules released at the start of the bit interval, while no molecules are released to send 0. The transmitter sends one information bit in the time interval T_{int} in order of the B-bit binary sequence $\mathbf{W} = \{W[1], W[2], ..., W[B]\}$, where $W[j]$ is the jth information bit and $P_r(W[j] = 1) = P_1$.

In our study, a time-varying electric field $\mathbf{E}(t)$ is applied uniformly to the entire system environment. The electric field induces an electrophoretic force $\mathbf{F}_E(t) = q_A\mathbf{E}(t)$ and it generates a flow of type-A molecules moving with a velocity of $\mathbf{v}(t)$, where q_A indicates the electric charge on a single type-A molecule. The electrophoretic force and the velocity of type-A molecules are assumed to be linearly proportional as verified in [8]; hence, $\mathbf{v}(t) \propto \mathbf{E}(t)$ also can be assumed. A time-varying velocity $\mathbf{v}(t)$ is composed of x, y, z directions, i.e., $\mathbf{v}(t) = (v_x(t), v_y(t), v_z(t))$. We consider the electric field in the x direction to push the molecules towards the receiver.

Also, we assume that the electric field is periodically applied whether a 0 or 1 is transmitted, i.e., no prior knowledge on the transmitted bits at the system level is required, and the electric field only affects electrically charged type-A molecules and does not affect the entire medium flow.

We indicate the concentration of type-A molecules transmitted at time t_0 at point $\mathbf{r}$ at time t as $C_A(\mathbf{r}, t; t_0)$ (molecules$\cdot$m^{-3}), or C_A for compactness. We assume the type-A molecules diffuse independently with a constant diffusion coefficient D_A(m^2/s).

B. Channel and Received Signal

The movement of molecules by advection and diffusion is expressed by Fick's second law [9] as

$$\frac{\partial C_A}{\partial t} + \mathbf{v}(t) \cdot \nabla C_A = D_A \nabla^2 C_A. \tag{1}$$

In an unbounded three-dimensional environment, the corresponding initial condition (IC) and the boundary condition (BC) are expressed as

$$\text{IC} : C_A(\mathbf{r}, t_0; t_0) = N_{EM}\delta(\mathbf{r} - \mathbf{r}_{TX}), \tag{2a}$$

$$\text{BC} : C_A(\mathbf{r} \to \infty, t; t_0) = 0. \tag{2b}$$

By applying these conditions to (1) and using a moving reference frame, the expected concentration of type-A molecules at point $\mathbf{r} = (x, y, z)$ at time $t \geq t_0$ is given by

$$C_A(\mathbf{r}, t; t_0) = \frac{N_{EM}}{(4\pi D_A(t - t_0))^{3/2}}\exp\left(-\frac{|\mathbf{r}_{eff}(t)|^2}{4D_A(t - t_0)}\right) \tag{3}$$

where

$$|\mathbf{r}_{eff}(t)|^2 = \left(x + x_0 - \int_{t_0}^t v_x(\tau)\,d\tau\right)^2 + \left(y - \int_{t_0}^t v_y(\tau)\,d\tau\right)^2$$
$$+ \left(z - \int_{t_0}^t v_z(\tau)\,d\tau\right)^2 \tag{4}$$

is the square of the effective distance from the transmitter to the point $\mathbf{r} = (x, y, z)$.

Then, the expected number of type-A molecules within the sphere receiver volume $\mathcal{V}_{obs}$ can be written as

$$\overline{N_{A_0}}(t; t_0) = \iiint_{\mathbf{r} \in \mathcal{V}_{obs}} C_A(\mathbf{r}, t; t_0)r^2 \sin\theta\,d\theta\,d\phi\,dr. \tag{5}$$

Then, by assuming that the concentration of type-A molecules in the entire receiver is identical to the concentration at the center of the receiver sphere, which is the so-called uniform concentration assumption [10], (5) can be simplified to

$$\overline{N_{A_0}}(t; t_0) = V_{obs}C_A((0, 0, 0), t; t_0). \tag{6}$$

The number of type-A molecules within the sphere receiver volume would be a Poisson random variable with mean $\overline{N_{A_0}}(t; t_0)$. Therefore, the total number of molecules observed – due to the transmission of the binary sequence $\mathbf{W}$ – $N_{A_{TX}}(t)$ is a Poisson random variable with mean

$$\overline{N_{A_{TX}}}(t) = \sum_{j=1}^{\left\lfloor \frac{t}{T_{int}} + 1 \right\rfloor} W[j]\overline{N_{A_0}}(t; (j - 1)T_{int}). \tag{7}$$

Assuming that type-A molecules diffuse randomly and independently, the total number of the instantaneously observed molecules $N_{\mathrm{obs}}(t)$, including noise molecules, is a sum of time-varying Poisson random variables with time-varying mean

$$\overline{N_{A_{\mathrm{obs}}}}(t) = \overline{N_{A_{\mathrm{TX}}}}(t) + \overline{N_{A_n}}(t) \tag{8}$$

where $\overline{N_{A_n}}(t)$ is the mean number of observed molecules due to the noise sources.

C. Weighted Sum Detectors

A common sampling scheme in which M-observations are made in every bit interval at the spherical receiver is utilized to model the detector. We assume the observations are made every constant period of t_s. We introduce $s_{j,m}$ as the value of the mth observation in the jth bit interval taken at time

$$t(j, m) = jT_{\mathrm{int}} + t_s m \tag{9}$$

where $j \in \{1, 2, ..., B\}$, $m \in \{1, 2, ..., M\}$. In addition, we utilize the weighted sum detector in [5], whose decision rule in the jth bit interval can be written as

$$\hat{W}[j] = \begin{cases} 1 & \text{if } \sum_{m=1}^{M} \omega_m N_{A_{\mathrm{obs}}}(t(j, m)) \geq \gamma, \\ 0 & \text{otherwise} \end{cases} \tag{10}$$

where ω_m and γ indicate the weight of the mth observation and the binary decision threshold, respectively. In this study, we set $\omega_m = \overline{N_{A_{\mathrm{obs}}}}(g(m))$, which is optimal in the sense that it maximizes the signal-to-noise ratio (SNR) and minimizes the BER, as analytically verified in [5].

III. DESIGNING PIECEWISE CONSTANT ELECTRIC FIELDS

To improve the BER performance, the MC receiver requires observing a higher number of the observed information-carrying molecules (i.e., the signal strength), while receiving a lower number of molecules remained from previous transmission (i.e., the ISI). Our previous work [8] utilized the electrophoretic force that changes as a form of an exponential or sinusoidal function to intentionally move the information-carrying molecules to achieve a better BER performance. However, such an exponential or sinusoidal electric field is hard and expensive to be implemented in some MC applications due to hardware or environmental limitations. Hence, we propose to use a piecewise constant electric field (i.e., velocity), which can be easily implemented via, e.g., an on/off switch method, to facilitate electrophoretic MC systems in practice.

Fig. 2 describes an example of the piecewise constant x-axis velocity $v_x(t)$. This work considers only the x-axis flow (so the only non-zero component of $\mathbf{v}(t)$ is $v_x(t)$) since the transmitter and receiver are aligned with the x-axis. $v_x(t)$ can be interpreted as the velocity of the center of the information-carrying molecule group, while the individual molecules randomly diffuse away from their center due to the Brownian motion. Once the molecules are injected into the channel at $t = 0$, the center of the molecule group moves from the transmitter to the receiver at the velocity v_1 during $t_0 \leq t < t_1$,
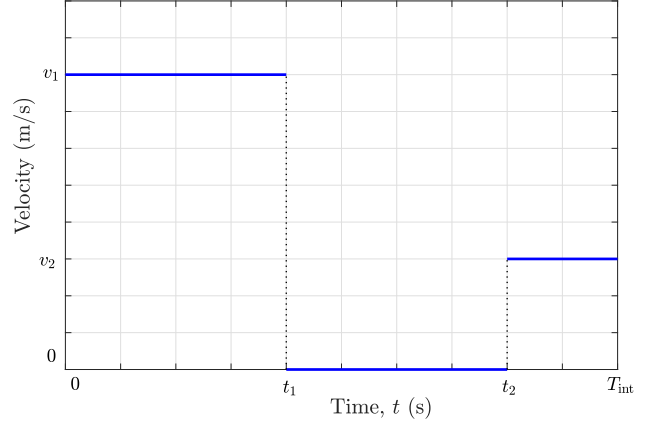

Fig. 2. The x-axis velocity of the center of the information-carrying molecule group $v_x(t)$ when the piecewise constant electric field is applied.

stays there (i.e., zero velocity) during $t_1 \leq t < t_2$, and leaves the receiver site with velocity v_2 during $t \geq t_2$. The first part velocity v_1 enables the information-carrying molecules to move toward the receiver site as quickly as possible, while the second one v_2 blows them away from the receiver. The zero-velocity during t_1 and t_2 allows the receiver to count the molecules with a high concentration.

Based on this framework, this section investigates the piecewise constant electric field designing the four parameters t_1, t_2, v_1, and v_2 to improve the BER performance. Two different optimization strategies are considered: the first is to minimize the MSE between the center of the molecule group and the receiver sphere given a bit interval time, and the second is to minimize a bit interval time given an observation time. Both problems are constrained by the average power of the electric field and the final location condition, which is closely related to the ISI component. Both approaches would be useful from the engineering perspective since engineers often might need to design an electric field from different system requirements.

A. Optimization Minimizing MSE

This section investigates the optimization problem of minimizing the MSE between the molecule group's center and the receiver sphere's center. The MSE indicates how closely the center of the molecule group is located to the receiver site; thus, we can design an electric field to locate the center of the molecule group at the receiver site as close and long as possible by minimizing the MSE. Eventually, the electric field with a lower MSE would allow a stronger information signal strength at the receiver site.

Therefore, we formulate an optimization problem with the MSE objective as

$$\underset{v_1, v_2, t_1, t_2}{\arg\min} \quad \frac{1}{T_{\mathrm{int}}} \int_0^{T_{\mathrm{int}}} (x(t) - x_0)^2 \, \mathrm{d}t \tag{11a}$$

$$\text{s. t.} \begin{cases} \dfrac{1}{T_{\mathrm{int}}} \displaystyle\int_0^{T_{\mathrm{int}}} v_x^2(t) \, \mathrm{d}t \leq \xi_v \\ \mathrm{IC} : x(0) = 0 \\ \mathrm{FC} : x(T_{\mathrm{int}}) = x_1 \end{cases} \tag{11b}$$

where $x(t) = \int_0^t v_x(\tau)\,d\tau$ denotes the distance between the center of the molecule group and the transmitter. The first constraint limits the average power of the electric field up to ξ_v. Note that constraining the mean value of the squared velocity is identical to constraining the average power of the electric field since $\mathbf{v}(t) \propto \mathbf{E}(t)$. The final condition FC is set to force the information molecules in the current bit interval away for the new group of molecules coming in the next bit interval. By controlling FC, we can balance the strengths of the information signal and the ISI component. In other words, if setting x_1 closer to the receiver sphere, the center of the molecule group can stay there until the end of the bit interval, allowing a higher number of the observed molecules. In contrast, the number of molecules remaining in the next bit interval would be more considerable. In addition, the final condition might be necessary to meet the design requirements of the MC application, e.g., the location of transducer/biosensor outlets.

Since analytically solving (11) with the four optimization variables is not straightforward, we make a reasonable assumption that the molecule group arrives at the center of the receiver sphere at t_1, that is, $v_1 t_1 = x_0$. This assumption also renders $v_2(T_{\text{int}} - t_2) = x_1 - x_0$ from FC in (11b). Then, by using these two equations, the objective function (11a) can be simplified to a function of the two optimization variables t_1, t_2:

$$f_{\text{obj}}(t_1, t_2) = \frac{1}{T_{\text{int}}} \left(\int_0^{t_1} (v_1 t - x_0)^2\, dt + \int_{t_2}^{T_{\text{int}}} v_2^2 (t - t_2)^2\, dt \right)$$
$$= \frac{1}{3 T_{\text{int}}} \left(x_0^2 t_1 + (x_1 - x_0)^2 (T_{\text{int}} - t_2) \right). \tag{12}$$

Also, in a similar manner, the first constraint of (11b) can be rewritten as

$$\frac{1}{T_{\text{int}}} \left(v_1^2 t_1 + v_2^2 (T_{\text{int}} - t_2) \right) = \frac{1}{T_{\text{int}}} \left(\frac{x_0^2}{t_1} + \frac{(x_1 - x_0)^2}{(T_{\text{int}} - t_2)} \right) \le \xi_v. \tag{13}$$

Since the initial and final conditions in (11b) are already taken into account in (12) and (13), the original optimization problem (11) can be transformed to

$$\underset{t_1, t_2}{\arg\min}\ f_{\text{obj}}(t_1, t_2) \tag{14a}$$

$$\text{s. t. } \frac{1}{T_{\text{int}}} \left(\frac{x_0^2}{t_1} + \frac{(x_1 - x_0)^2}{(T_{\text{int}} - t_2)} \right) \le \xi_v. \tag{14b}$$

Then, defining

$$g_{\text{cstr}}(t_1, t_2) = \frac{x_0^2}{t_1} + \frac{(x_1 - x_0)^2}{(T_{\text{int}} - t_2)} - \xi_v T_{\text{int}} \tag{15}$$

we form the Lagrangian [11] as follows

$$\mathcal{L} = f_{\text{obj}}(t_1, t_2) - \lambda g_{\text{cstr}}(t_1, t_2) \tag{16}$$

assuming $\lambda < 0$, where $\lambda \in \mathbb{R}$ is the Lagrange multiplier. Then, computing the partial derivative of $\mathcal{L}$ with respect to (t_1, t_2) and setting the result equal to zero leads to

$$\nabla f_{\text{obj}}(t_1, t_2) = \lambda \nabla g_{\text{cstr}}(t_1, t_2) \tag{17}$$

where

$$\nabla f_{\text{obj}}(t_1, t_2) = \frac{1}{3} T_{\text{int}} \left[x_0^2, \ -(x_1 - x_0)^2 \right],$$

$$\nabla g_{\text{cstr}}(t_1, t_2) = \left[-\left(\frac{x_0}{t_1} \right)^2, \ \left(\frac{x_1 - x_0}{T_{\text{int}} - t_2} \right)^2 \right].$$

By comparing both sides of (17), we can conclude that the optimal solutions t_1^*, t_2^* satisfy

$$t_1^* = \sqrt{-3 T_{\text{int}} \lambda},$$
$$t_2^* = T_{\text{int}} - \sqrt{-3 T_{\text{int}} \lambda} \tag{18}$$

which yields

$$t_2^* = T_{\text{int}} - t_1^*. \tag{19}$$

Then, the optimal solutions t_1^*, t_2^* can be calculated by plugging (19) into $g_{\text{cstr}}(t_1, t_2) = 0$. Finally, the optimal velocities v_1^*, v_2^* can be directly obtained from solving $v_1^* = x_0/t_1^*$, $v_2^* = (x_1 - x_0)/(T_{\text{int}} - t_2^*)$.

B. Optimization Minimizing Bit Interval

This subsection designs the electric field minimizing the bit interval time given a fixed observation time T_{ob}, which is the time duration that the center of the molecule stays at the center of the receiver sphere, i.e., $T_{\text{ob}} = t_2 - t_1$. Accordingly, the optimization problem can be formulated by

$$\underset{v_1, v_2, t_1, t_2, T_{\text{int}}}{\arg\min}\ T_{\text{int}} \tag{20a}$$

$$\text{s. t. } \begin{cases} \dfrac{1}{T_{\text{int}}} \displaystyle\int_0^{T_{\text{int}}} v_x^2(t)\, dt \le \xi_v \\ t_1 + T_{\text{ob}} + (T_{\text{int}} - t_2) \le T_{\text{int}} \\ v_1 t_1 = x_0 \\ \text{IC} : x(0) = 0 \\ \text{FC} : x(T_{\text{int}}) = x_1 \end{cases} \tag{20b}$$

where we can note the objective is to minimize the bit interval T_{int}. The first constraint limits the average power of the electric field, and the second and third constraints ensure the center of the molecule group stays at the receiver site for the duration T_{ob} as intended. Then, the initial and final conditions are constrained as in (11).

To facilitate solving the problem, we first transform (20) into a GP form, which can be made convex by means of a change of variables [12]. The first constraint can be solved as

$$\frac{1}{T_{\text{int}}} (v_1^2 t_1 + v_2^2 \Delta t_2) \le \xi_v \tag{21}$$

where $\Delta t_2 = T_{\text{int}} - t_2$, and the 3rd constraint and the IC and FC yield $x_0 + v_2 \Delta t_2 = x_1$. Then, (20) can be rewritten as

$$\underset{v_1, v_2, t_1, \Delta t_2, T_{\text{int}}}{\arg\min}\ T_{\text{int}} \tag{22a}$$

$$\text{s. t. } \begin{cases} \dfrac{1}{\xi_v} \left(v_1^2 t_1 T_{\text{int}}^{-1} + v_2^2 \Delta t_2 T_{\text{int}}^{-1} \right) \le 1 \\ (t_1 + T_{\text{ob}} + \Delta t_2) T_{\text{int}}^{-1} \le 1 \\ v_1 t_1 x_0^{-1} = 1 \\ (x_1 - x_0)^{-1} v_2 \Delta t_2 = 1. \end{cases} \tag{22b}$$

This problem is not convex itself, but a simple variable transformation $y_1 = \log t_1$, $y_2 = \log \Delta t_2$, $y_3 = \log v_1$, $y_4 =$
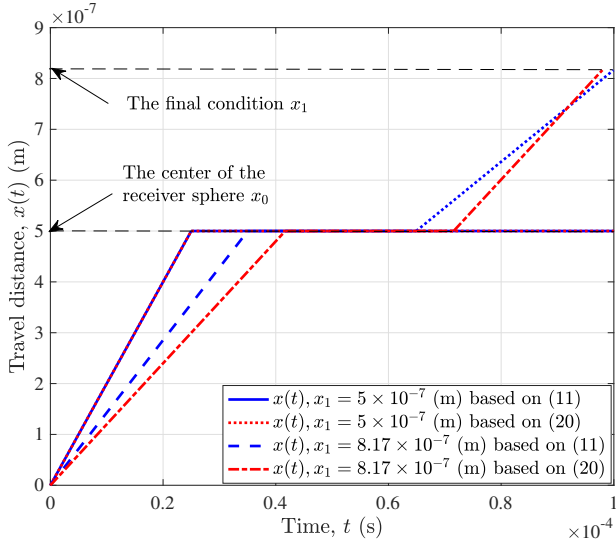
Fig. 3.   The travel distance of the center of the molecule group $x(t) = \int_0^t v_x(\tau)\,d\tau$ when the proposed velocities based on (11) and (20) with the different final conditions x_1 are induced. The observation times for (20) are set identical to the case of (11) as $T_{ob} = 0.75 \times 10^{-4}$ s and 0.30×10^{-4} s for $x_1 = 5 \times 10^{-7}$ m and 8.17×10^{-7} m, respectively.

Fig. 4.   The MSE, the bit interval time T_{int}, and the observation time T_{ob} for the different average power constraints ξ_v. T_{ob} is obtained when minimizing the MSE through (11), then is used for minimizing T_{int} through (20). Thus, T_{ob} for a given ξ_v is identically set for the results of the MSE with (11) and T_{int} with (20). $T_{int} = 0.1$ ms is used for (11).

$\log v_2$, and $y_5 = \log T_{int}$ allows to put this into an equivalent, convex form as

$$\underset{y_1, y_2, y_3, y_4, y_5}{\mathrm{argmin}} \quad y_5 \tag{23a}$$

$$\text{s. t.} \begin{cases} \log\left(\dfrac{1}{\xi_v}e^{y_1+2y_3-y_5} + \dfrac{1}{\xi_v}e^{y_2+2y_4-y_5}\right) \le 0 \\ \log\left(e^{y_1-y_5} + T_{ob}e^{-y_5} + e^{y_2-y_5}\right) \le 0 \\ y_1 + y_3 - \log x_0 = 0 \\ y_2 + y_4 - \log(x_1 - x_0) = 0. \end{cases} \tag{23b}$$

Note that all the objective and constraint functions are now convex; thus, its solutions $y_1^*, y_2^*, ..., y_5^*$ can be easily solved by using a standard optimization programming method like the sequential quadratic programming (SQP) algorithm [13]. Then, the final solutions can be calculated through $t_1^* = e^{y_1^*}$, $t_2^* = e^{y_2^*} + T_{int}$, $v_1^* = e^{y_3^*}$, $v_2^* = e^{y_4^*}$, $T_{int}^* = e^{y_5^*}$.

IV. OPTIMIZED FIELDS

This section explains how the two electric fields designed through the optimization problems (11) and (20), respectively, function in moving the center of the molecule group. Fig. 3 illustrates the center location of the molecular group, i.e., $x(t) = \int_0^t v_x(\tau)\,d\tau$, when the piecewise velocities designed with different final conditions $x_1 = 5 \times 10^{-7}$ and 8.17×10^{-7} are applied. The blue and red lines are the results for $x(t)$ with (11) and (20), respectively. Also, the observation times for (20) are set identical to the case of (11) as $T_{ob} = 0.75 \times 10^{-4}$ s and 0.30×10^{-4} s for $x_1 = 5 \times 10^{-7}$ m and 8.17×10^{-7} m, respectively.

For the final condition $x_1 = 5 \times 10^{-7}$ m, i.e., $x_1 = x_0$, both the molecule groups with (11) and (20) initially move at the velocity of $v_1 = 0.20$ m/s and reach the center of the receiver sphere at $t_1 = 0.25 \times 10^{-4}$ s. Then, the center of the molecule group stays there until the end of the bit interval
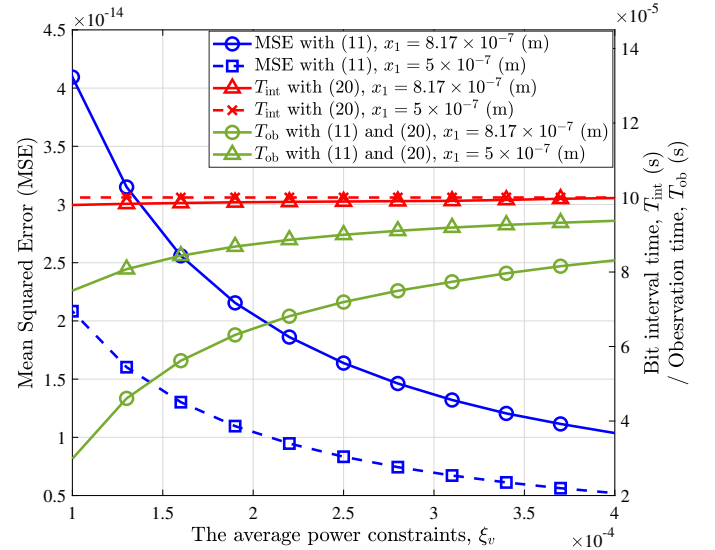
T_{int}. It is noted that by setting $x_1 = x_0$, both of the two electric fields designed by the optimization problems (11) and (20), respectively, perform in the identical way that they send the molecule group quickly toward the receiver sphere and make it remain there until the next bit interval. On the other hand, when the final condition is set as $x_1 = 8.17 \times 10^{-7}$ m, i.e., $x_1 > x_0$, the molecule groups rapidly move toward the receiver sphere, reach and stay there for a while, and move again toward the final condition location x_1. It is different from the previous case $x_1 = x_0$ that the molecule groups further moves toward x_1 after being located at x_0 to satisfy the final condition $x(T_{int}) = x_1$.

Regarding the difference between the optimization approaches in (11) and (20), we can note that the field based on (11) with $x_1 = 8.17 \times 10^{-7}$ m can locate the molecule group at the receiver sphere at $t_1 = 3.5 \times 10^{-5}$, earlier than that of (20) as $t_1 = 4.17 \times 10^{-5}$. The molecule group's earlier arrival at the receiver site under the field of (11) would allow a higher molecule concentration, which would result in stronger information signal strength. On the other hand, the field of (20) locates the molecule group at the final condition x_1 at $T_{int} = 0.98 \times 10^{-4}$ s, earlier than the bit time interval of (11) as $T_{int} = 0.1 \times 10^{-3}$ s. These results imply that the field designed based on (20) can minimize the bit interval time as intended, slightly sacrificing the initial velocity and the information signal strength, compared to (11).

Fig. 4 illustrates the MSE, the bit interval time T_{int}, and the observation time T_{ob} for the different average power constraints ξ_v. The MSE for a given value of ξ_v is minimized through solving (11), where we also obtain the observation time $T_{ob}^* = t_2^* - t_1^*$. Then, using the obtained T_{ob}^*, we solve (20) to minimize the bit time interval T_{int}. That is, the results with (11) and (20) for the same value of ξ_v have an identical observation
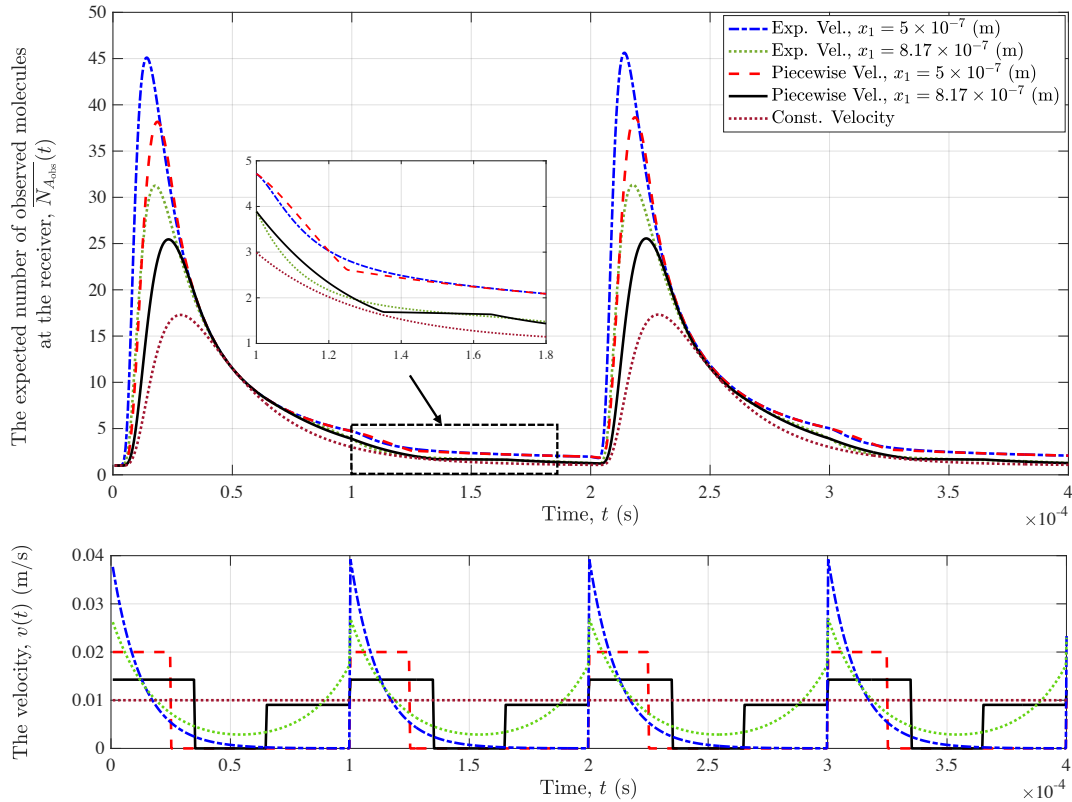
Fig. 5. The expected number of molecules observed within the passive receiver sphere $\overline{N_{A_{\text{obs}}}}(t)$ and x-axis velocity component $v_x(t)$ according to the different electric fields. $T_{\text{int}} = 0.1$ ms is used.

time T_{ob}. First, as shown in the figure, as the average power constraints ξ_v increases, the MSE decreases since the center of the molecule group more rapidly moves toward the receiver sphere and leaves there more quickly toward the final condition x_1 with a higher power constraint. Also, as discussed earlier, we can note a lower MSE corresponds to a longer observation time T_{ob}. On the one hand, T_{int} obtained from solving (20) slightly increases as ξ_v increase, but at most up to 0.1 ms, which is the bit time interval value that is used for solving (11). This result verifies that the approach (20) effectively minimizes the bit time interval T_{int} when the other parameters, such as T_{ob}, ξ_v, and x_1, are fixed.

On the one hand, note that this work utilizes only two segments in the piecewise field, but it is also possible to consider a more general piecewise field with more segments to approach the 'optimal' performance, i.e., exponential field. This should be possible in two different ways: (i) Increasing the number of segments will yield a finer tuning of the field, which will lower the objective functions (i.e., the MSE or the time interval) than the piecewise field only with two segments, and improve the BER performance. This approach increases the degrees of freedom in optimization problems, expanding the feasible set of solutions. (ii) One could instead begin with the *infinite resolution* scenario, i.e., the original exponential curve, and sample/quantize to obtain the discrete field profile. In this case, sampling/quantization introduces 'noise,' thus reducing the efficacy of the solution. Both approaches

TABLE I
SYSTEM PARAMETERS, ADOPTED FROM [8]

Parameter	Symbol	Value
Number of molecules per emission	N_{EM}	10^4
Probability of binary 1	P_1	0.5
Sampling interval	t_s	15 μs
Location of transmitter	x_0	0.5 μm
Radius of receiver	r_{obs}	50 nm
Length of transmitter sequence	B	100 bits
Diffusion coefficient	D_A	$10^{-9} m^2 s^{-1}$
Average power constrains	ξ_v	10^{-4}

would be effectively solved via various optimization methods. However, the field with a higher number of segments would sacrifice the simplicity of the piecewise electric field only with two segments in terms of implementation and mathematical complexity.

V. BIT-ERROR RATE RESULTS

In this section, we provide numerical results to verify the performances of the proposed piecewise constant electric field. The results for the proposed piecewise electric field based on (11)[1] and the benchmark fields – the constant field and the exponential field in [8] – are presented. The system parameters utilized for the simulations are given in Table I. For the

---

[1]Section IV reveals that there can be a little difference between the solutions obtained by (11) and (20); however, there is not a significant difference in BER performance since their physical mechanisms are identical.

simulation results, to avoid the high computational complexity of using the particle-based simulations, we generate Poisson random variables with time-varying mean $\overline{N_{A_{\text{obs}}}}(jT_{\text{int}} + t_s m)$ to mimic the observation value $s_{j,m}$ and then estimate the transmitted bit $W[j]$ according to the decision rule in (11). This simulation approach has already been validated in our previous work [8]. The simulation results were obtained through a Monte Carlo approach with 10^4 trials. The average power constraint $\xi_v = 10^{-4}$ is utilized such that the considered constant velocity ($v_x = 0.01$ m/s) has the same average squared value.

In Fig. 5, the top figure shows the expected number of observed molecules within the receiver volume $\overline{N_{A_{\text{obs}}}}(t)$ according to the time when the different types of electric fields (velocities) are applied. Also, the corresponding velocities $v(t)$ are shown in the bottom figure. We set an arbitrary transmitted binary sequence $\mathbf{W} = \{1, 0, 1, 0...\}$, and the result for only the first 4 bits is shown. In the top figure, we can note that the time-varying electric fields, i.e., the exponential and piecewise constant fields, yield higher peak numbers of the observed molecules (see the region of $0.1 \sim 0.3 \times 10^{-4}$s) than the constant velocity, while those of the piecewise constant velocities are slightly lower than the exponential field for the same x_1. On the other hand, the ISI for the exponential and piecewise constant fields are shown to be similar when the final condition x_1 is set identical (see the enlarged part in Fig. 5). Hence, the BER, which is affected by both the signal strength and ISI, for the different electric fields in the order of the figure legend is given as $\{0.27, 0.76, 0.59, 2.05, 4.57\} \times 10^{-3}$, respectively. It is noted that the proposed piecewise constant field yields worse BER performances (0.59×10^{-3} with $x_1 = 5 \times 10^{-7}$ m and 2.05×10^{-3} with $x_1 = 5 \times 10^{-7}$ m) than the exponential field (0.27×10^{-3} with $x_1 = 5 \times 10^{-7}$ m and 0.76×10^{-3} with $x_1 = 5 \times 10^{-7}$ m). Since the exponential velocity in [8] was designed without any field shape constraint unlike the proposed piecewise field, the exponential velocity can be expected to yield better performance than the proposed piecewise velocity. On the other hand, the piecewise fields are still much better BER performances than that of the constant field (4.57×10^{-3}). Also, the performance benefit of the proposed piecewise constant field can be considered satisfactory when considering its straightforward implementation complexity compared to the exponential field.

Fig. 6 illustrates the BER for different bit interval times T_{int}. In typical communication systems, the ISI decreases as the bit time interval increases; thus, the BER also improves. Similarly, the BER performances with the exponential and proposed piecewise constant velocities decrease as T_{int} increases since the ISI effect on the decoding is mitigated. On the other hand, comparing the results with the different final conditions x_1 shows that setting x_1 closer to the receiver (i.e., $x_1 = 5 \times 10^{-7}$ m) yields a better BER performance than setting it away from the receiver (i.e., $x_1 = 8.17 \times 10^{-7}$ m). Since this work considers an unbounded channel, there is enough room for the molecules to diffuse away from the receiver site as time elapses; thus, the ISI has little effect. Therefore, increasing the number of the observed information-carrying molecules at the receiver sphere by setting x_1 close to the receiver site is more
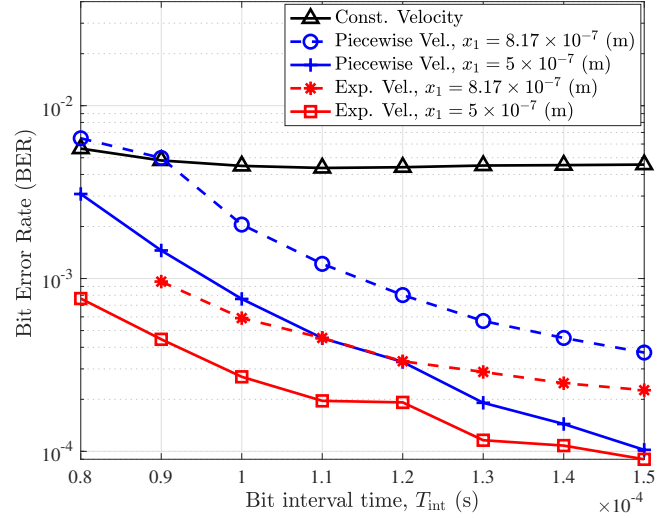

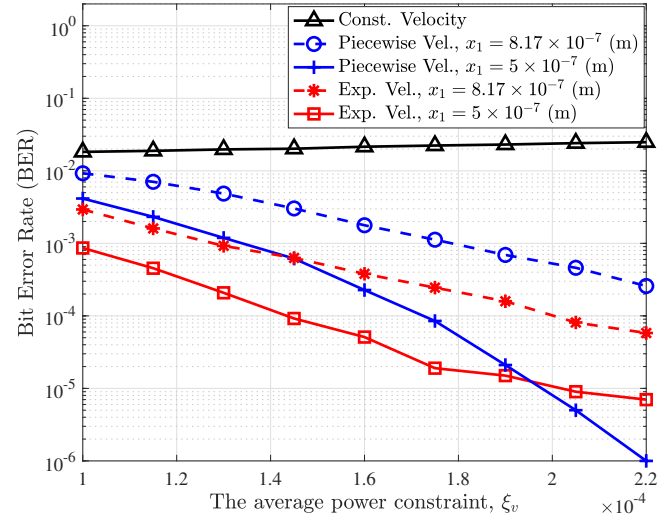Fig. 6. The BER performance for different bit interval times.

Fig. 7. The BER performance for different average power constraint. $T_{\text{int}} = 0.1$ s is used.

crucial than reducing the ISI effect by setting x_1 higher to achieve a better BER performance. In contrast, the BER with the constant velocity remains similar even as T_{int} increases because the ISI effect with the constant velocity is already little (see the region of $1.0 \sim 2.0 \times 10^{-4}$s in Fig. 5), compared to the other time-varying electric fields.

Fig. 7 illustrates the BER performance for different average power constraints, ξ_v. In section II-C, we assume that observation is made every constant period of t_s in (9). Hence, the BER performance with a constant electric field depends on the sampling time t_s; in other words, the BER performance appears good when the sampling is taken by chance when the center of the molecule group passes through the receiver sphere. On the one hand, the BER performances for the exponential and piecewise constant electric fields improve as the average power constraints ξ_v increase, regardless of
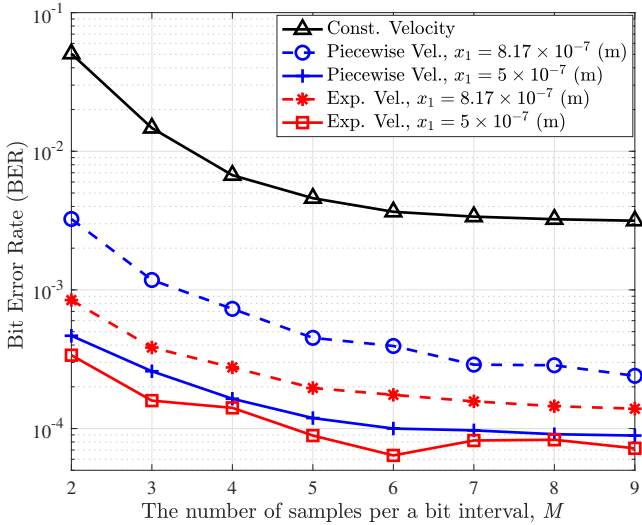
Fig. 8. The BER performance for different numbers of samples per a bit interval M. $T_{int} = 0.15$ s is used.

the sampling times. This enhancement is because, given the allowed average power ξ_v, the designed field locates the center of the molecule group toward the receiver sphere as quickly as possible and allows it to stay there until it has to move again to satisfy the final condition. That is, as the allowed power increases, the probability that the samplings are made when the center of the molecules stays at the receiver sphere also increases. Thus, the fact that the piecewise field does not need to carefully consider the observation timings t_s, unlike the constant field, can be an additional benefit from the engineering perspective.

Fig. 8 shows the BER performance for different numbers of samples per bit interval M. With all the electric fields, the BER decreases as M increases since the probability that the observations are taken when the number of the information-carrying molecules is high rises with a larger M, i.e., the weighted sum (10) increases (when binary 1 is transmitted).

In conclusion, the BER performances of the piecewise constant electric field in this work are meaningfully improved compared to the typical constant electric field but a bit lower than the performance of the exponentially changing electric field in [8]. This result can be comprehended when considering the much more straightforward implementation complexity of the piecewise constant field.

VI. CONCLUSION

This paper studied a novel framework of EMC systems utilizing a piecewise constant electric field to enhance communication performance. We introduced two optimization problems to design the electric fields based on different objectives: minimizing the MSE or the bit time interval. The problems were solved to find the optimal timing and field strength parameters using the Lagrange multiplier approach and GP method, respectively. The proposed electric field designs were shown to allow the information-carrying molecules to propagate rapidly and stay longer in the center of the receiver sphere,

consequently increasing the expected number of the observed molecules. Numerical results were provided to illustrate that the proposed EMC framework improves the BER performance.

REFERENCES

[1] N. Farsad, H. B. Yilmaz, A. Eckford, C. Chae, and W. Guo, "A comprehensive survey of recent advancements in molecular communication," *IEEE Commun. Surv. Tutorials*, vol. 18, no. 3, pp. 1887–1919, 2016.

[2] V. Jamali, A. Ahmadzadeh, W. Wicke, A. Noel, and R. Schober, "Channel modeling for diffusive molecular communication—a tutorial review," *Proc. IEEE*, vol. 107, no. 7, pp. 1256–1301, 2019.

[3] I. F. Akyildiz, F. Brunetti, and C. Blázquez, "Nanonetworks: A new communication paradigm," *Comput. Netw.*, vol. 52, no. 12, pp. 2260–2279, 2008.

[4] K. V. Srinivas, A. W. Eckford, and R. S. Adve, "Molecular communication in fluid media: The additive inverse gaussian noise channel," *IEEE Trans. Inf. Theory*, vol. 58, no. 7, pp. 4678–4692, 2012.

[5] A. Noel, K. C. Cheung, and R. Schober, "Optimal receiver design for diffusive molecular communication with flow and additive noise," *IEEE Trans. Nanobiosci.*, vol. 13, no. 3, pp. 350–362, 2014.

[6] V. Jamali, N. Farsad, R. Schober, and A. Goldsmith, "Non-coherent detection for diffusive molecular communication systems," *IEEE Trans. Commun.*, vol. 66, no. 6, pp. 2515–2531, 2018.

[7] I. F. Akyildiz, M. Pierobon, and S. Balasubramaniam, "An information theoretic framework to analyze molecular communication systems based on statistical mechanics," *Proc. IEEE*, vol. 107, no. 7, pp. 1230–1255, 2019.

[8] S. Cho, T. C. Sykes, J. P. Coon, and A. A. Castrejón-Pita, "Electrophoretic molecular communication with time-varying electric fields," *Nano Commun. Netw.*, vol. 31, p. 100381, 2022.

[9] H. C. Berg, *Random walks in biology*. Princeton University Press, 2018.

[10] A. Noel, K. C. Cheung, and R. Schober, "Using dimensional analysis to assess scalability and accuracy in molecular communication," in *2013 IEEE ICC in Budapest, Hungary*, June 2013, pp. 818–823.

[11] S. Boyd and L. Vandenberghe, *Convex optimization*. Cambridge university press, 2004.

[12] S. Boyd, S.-J. Kim, L. Vandenberghe, and A. Hassibi, "A tutorial on geometric programming," *Optimization and Engineering*, vol. 8, no. 1, pp. 67–127, 2007.

[13] P. T. Boggs and J. W. Tolle, "Sequential quadratic programming," *Acta Numerica*, vol. 4, p. 1–51, 1995.